A STOCHASTIC APPROACH TO AUTOMATED RECONSTRUCTION OF 3D MODELS OF INTERIOR SPACES FROM POINT CLOUDS

H. Tran [a, *] and K. Khoshelham [a]

[a] Department of Infrastructure Engineering, University of Melbourne, Parkville 3010, Australia - tran5@student.unimelb.edu.au, k.khoshelham@unimelb.edu.au

KEY WORDS: Indoor modelling, Point cloud, Automation, reversible jump Markov Chain Monte Carlor (rjMCMC), Metropolis – Hastings (MH), Building Information Model (BIM).

ABSTRACT:

Automated reconstruction of 3D interior models has recently been a topic of intensive research due to its wide range of applications in Architecture, Engineering, and Construction. However, generation of the 3D models from LiDAR data and/or RGB-D data is challenged by not only the complexity of building geometries, but also the presence of clutters and the inevitable defects of the input data. In this paper, we propose a stochastic approach for automatic reconstruction of 3D models of interior spaces from point clouds, which is applicable to both Manhattan and non-Manhattan world buildings. The building interior is first partitioned into a set of 3D shapes as an arrangement of permanent structures. An optimization process is then applied to search for the most probable model as the optimal configuration of the 3D shapes using the reversible jump Markov Chain Monte Carlo (rjMCMC) sampling with the Metropolis-Hastings algorithm. This optimization is not based only on the input data, but also takes into account the intermediate stages of the model during the modelling process. Consequently, it enhances the robustness of the proposed approach to inaccuracy and incompleteness of the point cloud. The feasibility of the proposed approach is evaluated on a synthetic and an ISPRS benchmark dataset.

1. INTRODUCTION

As-is three dimensional (3D) models of building interiors are of paramount importance for a variety of applications such as building management, indoor navigation, location-based services, and emergency responses. However, existing interior models are often not up-to-date, and therefore, do not represent the as-is condition of the buildings. Lidar scanning and photogrammetry are the two main techniques, which can effectively capture the as-is representation of a building (Khoshelham, 2018). However, a manual reconstruction of a 3D interior model from these data is a time-consuming, tedious, and error-prone task. An automatic approach, which is efficient in time and cost, for generation of the 3D models from the data (e.g., point clouds, images) is therefore needed. Yet, the automated reconstruction generally suffers from not only the complexity of building geometry, but also the presence of clutters in the indoor environment and the defects of input data.

In the literature, the approaches to reconstruction of a 3D model of a building interior from a point cloud either rely on local properties of the input data (Tran et al., 2017; Díaz-Vilariño et al., 2015; Xiong et al., 2013) or are based on global knowledge on the model plausibility with respect to the data and the interrelation between building elements (Mura et al., 2016; Ochmann et al., 2016). In practice, each strategy has its own pros and cons. The local approaches are generally efficient with the high-quality input data. Meanwhile, the global approaches are likely to enhance the global plausibility of the model with lower-quality data. However, the reconstruction of elements captured with high-quality can fail due to the influence of irrelevant lower-quality data points.

In this paper, we propose a stochastic approach to reconstruct volumetric models of interior spaces from point clouds using the reversible jump Markov Chain Monte Carlo (rjMCMC) sampling with Metropolis-Hastings algorithm (MH) (Hastings, 1970). The idea is, in addition to the input data, the intermediate stages of a model can be beneficial to the reconstruction of its final model. The main contribution of our approach is the integration of both local properties of the input data and the global knowledge on the model's plausibility as well as taking advantage of intermediate stages of a model in the 3D reconstruction process.

The following sections provide a review of related works (Section 2. Literature review) followed by a detailed description of the proposed method (Section 3. Methodology), and the experiments and results (Section 4. Experiments and Results).

2. LITERATURE REVIEW

Reconstruction of as-is 3D interior models from point cloud has been an intensive research topic in recent years (Pătrăucean et al., 2015). There are approaches for reconstructing the 3D models of building interior based on the interpretation of local properties of input data (Budroni and Böhm, 2010; Adan and Huber, 2011; Sanchez and Zakhor, 2012). For example, Sanchez and Zakhor (2012) reconstruct surface-based models of Manhattan-world buildings from point clouds by first classifying the data points into different building structures (i.e., walls, ceilings, and floors) using the point normals, followed by the application of plane-fitting to locally estimate the geometry of each building surface individually. Several researchers favour the combination of local features of input data and contextual knowledge to model each building elements separately (Khoshelham and Díaz-Vilariño, 2014; Hong et al., 2015; Macher et al., 2017). Xiong et al. (2013) applies a region-growing algorithm to extract planar surfaces of building interiors from voxelized data. The semantic information is then added using surfaces' local features (e.g., point density,

* Corresponding author

dimension, orientation) and the constraints on their contextual relationships (e.g., parallelism, orthogonality) with their neighbours. Similarly, in Nikoohemat et al. (2018) the semantics and geometries of building elements are derived from points belonging to each planar surface and the adjacency relationship between the surfaces. Khoshelham and Díaz-Vilariño (2014) and Tran et al. (2018) take into account the presence of points on surfaces of cuboid shapes and the spatial relationship with neighbours to classify a cuboid as a navigable space (i.e., rooms, corridors) or a non-navigable space (i.e., walls, ceilings/floors, exteriors) by iterative application of shape grammar rules. In general, the local approaches strongly depend on the data quality, and are suitable for the reconstruction of buildings which are well observable and are captured with high-quality data. These methods are less successful when applied to data with varying point density and high levels of occlusion and are likely to be more susceptible to clutter. Unfortunately, these are common features of data captured in most building interiors.

Several methods have been developed to reconstruct 3D interior models from point clouds by taking advantage of the global plausibility of the models with respect to the input data and interrelation between building elements (Oesau et al., 2014; Mura et al., 2016; Ochmann et al., 2016). Oesau et al. (2014) proposes an approach which can be applied to both Manhattan and Non-Manhattan architectures. The authors formulate the 3D interior modelling as a binary classification of building sub-spaces into solid cells (i.e., building elements, exteriors) and empty spaces (i.e., rooms, corridors). The classification is defined as a global minimization problem, which is solved by using a graph-cut algorithm. The global objective function is formulated as the combination of data faithfulness and model complexity. Similarly, Mura et al. (2016) reconstruct volumetric models by solving a multi-label optimization problem. The energy function is based on the visibility overlaps from different viewpoints of each sub-space and the areas covered by data points between two adjacent ones. Ochmann et al. (2016) propose to reconstruct building layouts and permanent structures of building interiors from point clouds by classifying their 2D floor regions into inside or outside areas. The classification is formulated as a minimization optimization problem, in which the global energy function is defined based on the projections of input point clouds on each floor region and the supporting points of the surfaces separating two adjacent cells.

The advantage of the global approaches lies in the consideration of the global plausibility of the output models with respect to input data and the interrelation between building elements. In practice, compared to local approaches, global approaches are likely to be more robust to the defects of input data due to the consideration of the model plausibility in the reconstruction process. For example, an interior sub-space of a building may be classified as an exterior space in a local approach due to the lack of points on its surfaces, while it can be correctly modelled as an interior cell in a global approach since it is connected to other interior sub-spaces and there are no actual surfaces separating them. However, global approaches treat the data with varied quality (i.e., point density, occlusions) equally. In addition, the influence of irrelevant low-quality data capturing one building part on the reconstruction of other building parts can hamper the quality of output models. This can be seen in the case of an interior cell covered with data points which can be labelled as exterior due to its connectivity relations with other cells having no supporting points.

Stochastic methods such as rjMCMC and MCMC algorithms have been used quite successfully for 3D modelling of objects in various applications. Oude Elberink and Khoshelham (2015) and Oude Elberink et al. (2013) used MCMC with MH algorithm to integrate local and global geometric properties of pieces of rails to model long rail tracks from point clouds. Schmidt et al. (2017) proposed a method to extract networks from raster data using rjMCMC process. Ripperda and colleagues applied the rjMCMC algorithm to reconstruct building façades in a series of papers (Ripperda, 2007; Ripperda and Brenner, 2008, 2009). Merrell et al. (2010) used rjMCMC to optimize the floor plans of residential buildings. In this paper, we propose a stochastic approach to reconstruct building spaces from point clouds using the rjMCMC sampling with MH algorithm. Our strategy is to integrate local properties of input data and model global plausibility by taking advantage of intermediate stages of a model in the reconstruction process.

3. METHODOLOGY

Our approach to reconstructing 3D models of interior spaces from point cloud consists of two main steps: space partitioning and model optimization. In the space partitioning step, the indoor scene is first partitioned into a set of volumetric cells as the arrangement of potential permanent building structures. Meanwhile, the model optimization step aims at finding the optimal configuration of the indoor model, in which each cell is classified as a navigable space or a non-navigable space using the rjMCMC with Metropolis-Hastings sampling algorithm (Hastings, 1970). The final model of an interior space is a union of its final navigable spaces (i.e., rooms, corridors).

3.1 Space partitioning

The point cloud is first segmented into vertical points, which are likely to belong to vertical structures (i.e., walls), and horizontal points, which potentially belong to horizontal structures (i.e., floors, ceilings) by using the point normal. A point is classified as a vertical point or a horizontal point if it has the normal n_p , which are parallel with the vertical direction or horizontal direction, respectively, up to a certain angle θ. The horizontal and the vertical structures are then extracted from horizontal points and vertical points separately by using the Random Sample Consensus plane-fitting algorithm (Schnabel., 2007) to reduce the influence of clutters and to eliminate the involvement of irrelevant points in the extraction of permanent structures. Each extracted plane must have a considerable number of supporting points to be considered as a building structure. Fig. 1 shows an example of a point cloud and the extraction results of horizontal and vertical planar structures of a building interior.

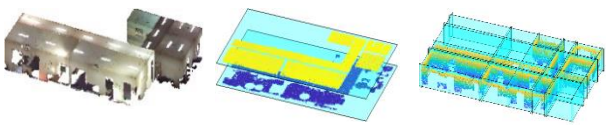

(a) (b) (c)

Fig. 1: Extraction of potential permanent structures of a building interior: (a) a point cloud as input data, (b) extraction of horizontal structures from horizontal points, (c) extraction of vertical structures from vertical points.

The interior space is partitioned into a set of 3D shapes formed by the intersection between the vertical plane segments and horizontal plane segments, which are limited by the bounding box of the point cloud. Fig. 2 illustrates the intersection between the vertical planar structures and horizontal structures to generate 3D decomposition of the building space.

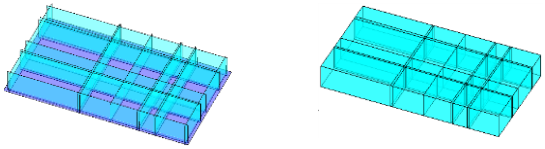

(a) (b)

Fig. 2 An illustration of 3D decomposition of an interior space: (a) intersection between horizontal and vertical structures (the ceiling plane has been removed for a better visualization), (b) the 3D decomposition.

The geometry of each shape is represented with a boundary representation $\{V, F\}$, where V is the set of vertices and F is its bounding faces. Meanwhile, the semantic information is stored as an attribute *type* indicating whether the shape is navigable ($type = 1$) or non-navigable ($type = 0$). At the space partitioning step, each shape has no semantic information ($type = \emptyset$).

3.2 Model configuration

The 3D model of an interior space is a set of cells comprising both the geometric $\{V, F\}$ and semantic $\{type\}$ information. An interior model is considered as the union of navigable spaces (i.e., rooms, corridors) of a building space. We define the number of shapes, the shape geometry $\{V, F\}$, and the sematic information $\{type\}$ as the parameters of a model. The reconstruction of an interior space is to search the optimal configuration of the model parameters, which vary in relation to possible changes in the 3D model and a joint probability distribution.

3.2.1. Transitions in the model configuration: we define four transitions likely to occur between two models in the space of all possible 3D models of a building interior:

(1) adding: a shape which has no semantic information ($type = \emptyset$), and is not in adjacency relationship with any navigable space is labelled as a navigable space ($type = 1$);

(2) removing: a navigable space ($type = 1$) which is not adjacent with any navigable space is changed to a shape with empty semantics ($type = \emptyset$);

(3) adding and merging: a shape which has no semantic information ($type = \emptyset$) is labelled as a navigable space ($type = 1$), and is then merge with its adjacent navigable spaces to form a new navigable space;

(4) splitting and removing: This is the reciprocal of the transition in (3). A navigable space which was formed by merging two or more navigable spaces is split into its components, and the $type$ of the navigable space which is added before the merging is changed to $type = \emptyset$.

With these defined transitions, we allow the changes of not only geometries and semantics, but also the number of shapes in the proposed 3D models. Fig. 3 gives examples of the transitions between two 3D models of an interior space.

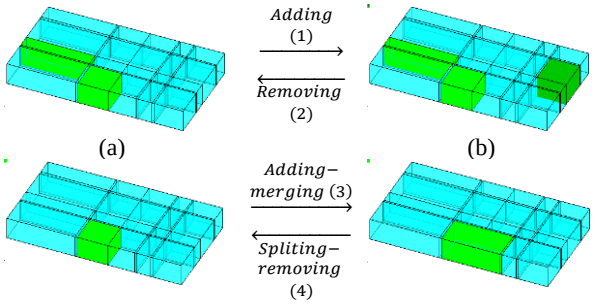

Fig. 3 Examples of transitions between two models in the model space of an interior space. Adding: from (a) to (b) by adding a navigable shape (dark green). Removing: from (b) to (a) by removing a navigable shape (dark green). Adding and merging: from (c) to (d) by adding a navigable shape and merging it with the adjacent space. Splitting and removing: from (d) to (c) by splitting a merged navigable space and nulling the semantics of one component.

3.2.2. Model probability function: We aim at reconstructing the most probable 3D model M of an interior space from given data D. According to Bayes' rule, the probability $P(M|D)$ of a model M given an input data D is proportional to the product of likelihood $P(D|M)$ and the prior $P(M)$: $P(M|D) \propto P(D|M)P(M)$. We define the prior $P(M)$ as a uniform distribution. This means without any data all models are considered equally likely and we do not prefer one model over another. Meanwhile, the likelihood $P(D|M)$ is defined as a joint probability distribution of the local likelihood $P_L(D|M)$ and the global likelihood $P_G(D|M)$: $P(D|M) = P_L(D|M)\,P_G(D|M)$. The details of these terms are described as follows:

Local likelihood: The local likelihood $P_L(D|M)$ is defined based on the local knowledge and the interpretation from the data enclosed in each individual shape. In general, a shape, which has points covering its top surface (i.e., ceiling) is likely to be a navigable space (Tran et al., 2018). Otherwise, the shape potentially represents a non-navigable space. We therefore formulate the local likelihood as follows:

$$P_L(D|M) = \prod_{i=1}^{n} \frac{Cov(M(i).top)}{Area(M(i).top)} \quad (1)$$

Where n is the number of navigable spaces in the model M. $Area(M(i).top)$ denotes the area of the top surface of a navigable shape $M(i)$. Meanwhile, $Cov(M(i).top)$ denotes the area of the top surface of $M(i)$ that is covered by points. This area is computed as the area of the 2D alpha-shape (Edelsbrunner and Mücke, 1994) derived from the Delaunay triangulation of the projection of data points on the top surface for each shape (Tran and Khoshelham, 2019).

The local likelihood $P_L(D|M)$ ranges from 0, indicating that the proposed model has at least one navigable space without supporting points, to 1, indicating that all the navigable spaces are totally covered by the input point cloud.

Global likelihood: The global likelihood $P_G(D|M)$ is defined to measure the fitness of the model M to the input data D and the model plausibility with respect to the data. We define the global likelihood as the combination of three data terms, i.e., horizontal fitness $P_{h_{cov}}$, vertical fitness $P_{v_{cov}}$, and model plausibility P_p as follows:

$$P_G(D|M) = \lambda_1 P_{h_{cov}} + \lambda_2 P_{v_{cov}} + \lambda_3 P_p \quad (2)$$

$\lambda_1, \lambda_2, \lambda_3$ are the normalization factors, which are used to weight the contribution of each term to the global likelihood and satisfy the condition $\lambda_1 + \lambda_2 + \lambda_3 = 1$.

Horizontal fitness: The horizontal fitness measures how well the horizontal structures of the proposed model fit the horizontal structures of the building space captured in the input point cloud. For each proposed model, we first measure the point coverage of the top surfaces of navigable spaces, so called horizontal coverage $M_{h_{cov}}$:

$$M_{h_{cov}} = \sum_{i=1}^{n} Cov(M(i).top) \quad (3)$$

Where n is the number of navigable spaces in the proposed model.

The horizontal fitness $P_{h_{cov}}$ is obtained by the normalization of the horizontal coverage $M_{h_{cov}}$ and is computed as the ratio of the coverage $M_{h_{cov}}$ to the total of the horizontal areas of the building, which is covered by the horizontal points $hpoints$:

$$P_{h_{cov}} = \frac{M_{h_{cov}}}{area(hpoints)} \quad (4)$$

Vertical fitness: Akin to horizontal fitness, the vertical fitness is measured based on the vertical coverage $M_{v_{cov}}$. The coverage $M_{v_{cov}}$ is computed as the area of side surfaces (i.e., wall surfaces) which is covered by the input point cloud, summed over all navigable spaces of a proposed model:

$$M_{v_{cov}} = \sum_{i=1}^{n} Cov(M(i).sides) \quad (5)$$

We normalize the vertical coverage to formulate the vertical fitness as the proportion of the vertical coverage in the proposed model to the total area of the vertical structures of the building which is supported by all the vertical data points $vpoints$:

$$P_{v_{cov}} = \frac{M_{v_{cov}}}{area(vpoints)} \quad (6)$$

Model plausibility: In addition to the surface coverages, which are encoded in the horizontal and vertical fitness terms, we measure the reliability and plausibility of the proposed model by measuring the areas covered by points (both horizontal and vertical), which fall inside the navigable spaces and therefore do not represent the vertical or horizontal structures. The more vertical and horizontal areas covered by inside points, the lower the model plausibility is. We formulate the model plausibility as follows:

$$P_p = 1 - \frac{\sum_{i=1}^{n} area(M(i).inPoints)}{area(hpoints) + area(vpoints)} \quad (7)$$

Where $M(i).inPoints$ is the vertical and horizontal points which fall inside the navigable space $M(i)$.

The value of P_p may be influenced in the environments with a high level of clutter. In these cases, the contribution of the model plausibility P_p to the global likelihood should be small, and it can be adjusted by reducing the value of its normalization factor λ_3 in Eq. (2).

3.3 Model optimization

The model optimization is to search for the most probable model in the space of all possible models of a building space with a given input data. We adapt the rjMCMC with the Metropolis-Hastings algorithm (Hastings, 1970) to solve this problem, as it is suitable for searching in the space of models with unknown distribution and when the set of model parameters varies (see section 3.2.1).

The rjMCMC with the MH algorithm simulates a discrete Markov Chain based on random walks on the model configuration spaces. The process starts with the 3D model, called the *starting* model M_0, which contains a navigable space having the highest local likelihood. Whether a jump from a current model M_t to the next proposed model M_{t+1} is accepted or not depends on the acceptance probability α. In other words, the modelling process is based on not only input data, but also the intermediate stages of the model. The general workflow, the transition kernel *J* from one model to another, and the formula of the acceptance probability α are described as follows.

The general workflow of the rjMCMC sampler with MH algorithm contains three main steps:

(1) Initialisation: *starting* model M_0 $(t = 0)$

(2) Iteration:

- Generate a proposed model M_{t+1} by sampling model transitions according to a predefined transition kernel $J(M_{t+1}|M_t)$
- Computing the acceptance probability α

$$\alpha = min\left\{1, \frac{p(M_{t+1}|D) \cdot J(M_{t+1}|M_t)}{p(M_t|D) \cdot J(M_t|M_{t+1})}\right\} \quad (8)$$

- Generate a uniform random number $U \in [\beta, 1]$ with $\beta \geq 0$
- Decide to accept (if $\alpha \geq U$) or to reject (if $\alpha < U$) a jump from the current model M_t to the proposed model M_{t+1}
- Set M_{t+1} as the current model

(3) End: The process is ended when it reaches a predefined number of iterations

We introduce a new parameter $\beta \geq 0$, called a convergence parameter, in the generation of a uniform random number U to allow users flexibility to search for the most probable model either in the sub-space of models, which has high probability, or in the whole model space as default. This way ensures that the proposed model satisfies a certain level of quality. Thus, it facilitates a faster convergence of the optimization process as well as reducing the influence of incompleteness and inaccuracy of data on the proposed model. However, deciding a suitable value for β is important as the high value of β may lead to a local optimum instead of a global optimum.

The transition kernel $J(M_{t+1}|M_t)$ represents the probability for the change from the current model to the next proposed model. We adapt the concept of minimum description length (Rissanen, 1978) to define the transition kernel. As the final model is formed as the union of the final navigable spaces (i.e., rooms, corridors), we define the transition kernel based on the number of the final navigable spaces of the model. In other words, we consider the complexity of a 3D model into the reconstruction process. The final model should be the most compact model, which is not only the most fitted to the input data, but also has the smallest number of final navigable spaces (i.e., rooms, corridors) as the result of

the condition that all the adjacent spaces should be merged to form a unified navigable space.

We formulate the complexity of a model as:

$$C(M) = log_2^n \quad (9)$$

Where n is the number of navigable spaces in the model M. $C(M) = 1$, when $n = 1$.

The transition kernel $J(M_{t+1}|M_t)$ is defined as follows:

$$J(M_{t+1}|M_t) = \frac{C(M_t)}{C(M_{t+1})} \quad (10)$$

The optimization process is to reconstruct final navigable spaces of a building interior. Once the process is finished, all the 3D shapes which are not classified as navigable spaces will be automatically assigned as non-navigable spaces $type = 0$. The sampled models are ranked according to the model probabilities. The user interactions can select the best model among the most probable models sampled from the space of all possible models of an indoor space.

4. EXPERIMENTS AND RESULTS

Experiments with a synthetic dataset and an ISPRS benchmark dataset were conducted to evaluate the feasibility of the proposed method for the reconstruction of 3D models of interior spaces with different architectures (i.e., Manhattan and Non-Manhattan designs) from point clouds.

The synthetic dataset represents a hexagon building comprising a connected and large hall. The building has a large exterior space with several small plants and a tree surrounded by the walls. The synthetic point cloud was created with an average point spacing of 5 cm with low level of noise. The real dataset TUB1 from the ISPRS benchmark dataset was captured by a Viametris iMS3D mobile scanning system with a nominal accuracy of 3 cm (Khoshelham et al., 2017). The dataset represents a large Manhattan building with the presence of clutters and moving objects (i.e., people). The normalization parameters λ_1, λ_2, λ_3 are set to $1/3$ empirically in both experiments. The convergence parameter β is set to 0.2 and 0.1 for the experiments on the synthetic and real datasets respectively.

4.1 Results for the synthetic dataset

The synthetic point cloud of a hexagon building was first segmented into horizontal points and vertical points, from which the potential building surfaces can be extracted. Fig. 4 shows the input point cloud, potential surfaces of the floor and the ceiling, and the potential wall surfaces.

Fig.5(a) shows the cell decomposition of the building space, which comprises 89 shapes in total. As can be seen from the figure, the hall of the building space is partitioned into 24 individual shapes. In the reconstruction process, these 3D shapes are classified as navigable spaces. Those spaces which are adjacent to each other will iteratively be merged together to form the final unified navigable space, i.e., the large hall. Fig. 5(b) shows the classification results containing both navigable spaces (green) and non-navigable spaces (light pink). The final model containing a final navigable space, which corresponds to the large and connected hall of the environment, is shown in Fig. 5(c). The final model was selected by users among the sampled models ranked with the highest model probabilities. The large exterior with the plants and tree, surrounded by walls, is not classified as an interior navigable space (i.e., rooms, corridors) as there is no point on its top surface, and as it is separated from other navigable spaces by walls.

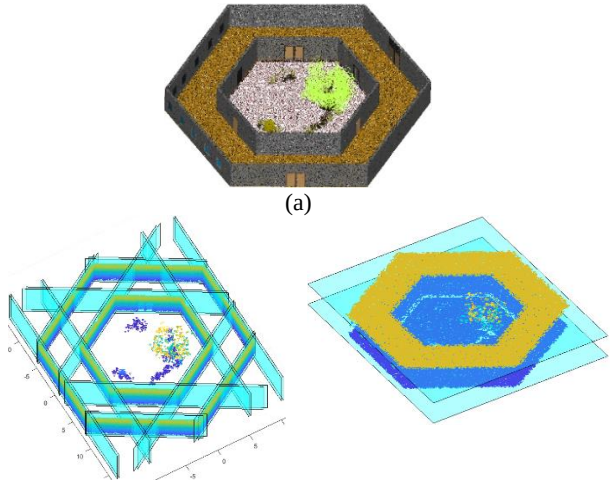

(a) (b) (c)

Fig. 4. Extraction of potential building structures of the synthetic building: (a) synthetic point cloud (the ceiling is removed for better visualization), (b) vertical structures, i.e., walls, (c) horizontal structures, i.e., the ceiling and the floor.

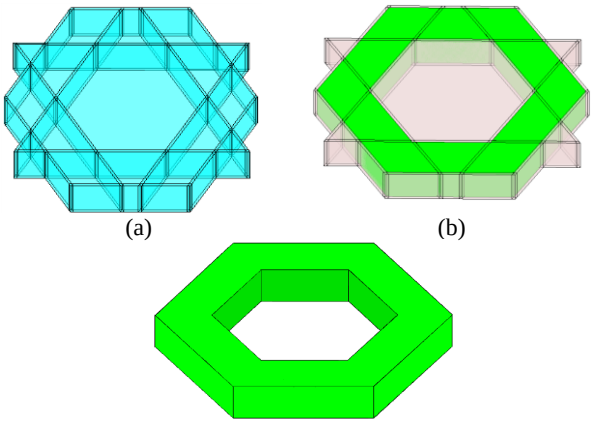

(a) (b) (c)

Fig. 5. Results for the synthetic dataset: (a) 3D cell decomposition, (b) the classification of cells into navigable spaces (green) and non-navigable spaces (light pink), (c) the final model.

4.2 Results for the ISPRS benchmark dataset

The real point cloud represents the TUB1 building from the ISPRS benchmark dataset, which contains a long corridor and 9 separate rooms. The quality of the point cloud varies in different parts of the building. In the data, several rooms are completely captured, while parts of the building are partially presented in the data.

Fig. 6 shows the point cloud, the horizontal planes of the ceiling and the floor, and vertical planes representing wall surfaces. Each extracted plane must have at least 80 supporting points to be considered as a building structure in this experiment. There are totally two horizontal planes (i.e., the ceiling and the floor) and 32 vertical planes, which are then used to form the cell decomposition of the building space.

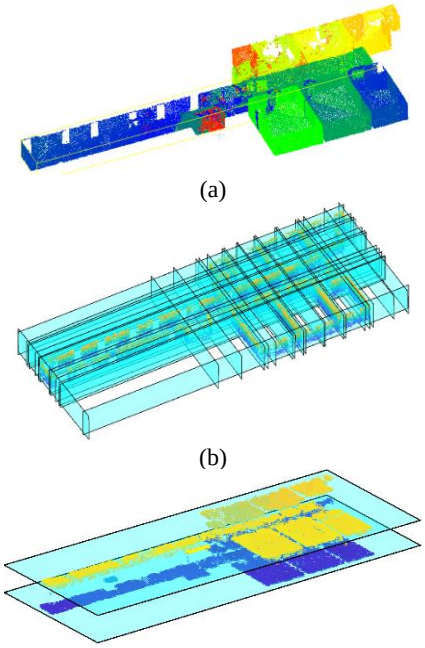

(a) (b) (c)

Fig. 6. Extraction of building structures of the TUB1 building: (a) the point cloud (the ceiling is removed for a better visualization), (b) vertical structures (c) horizontal structures.

Fig. 7 shows the reconstruction results for the TUB1 dataset of the ISPRS benchmark datasets. The environment is partitioned into 216 individual cells (Fig.7a), which are then classified into navigable spaces (green) and non-navigable spaces (light pink) (Fig.7b) to form the final model (Fig. 7c).

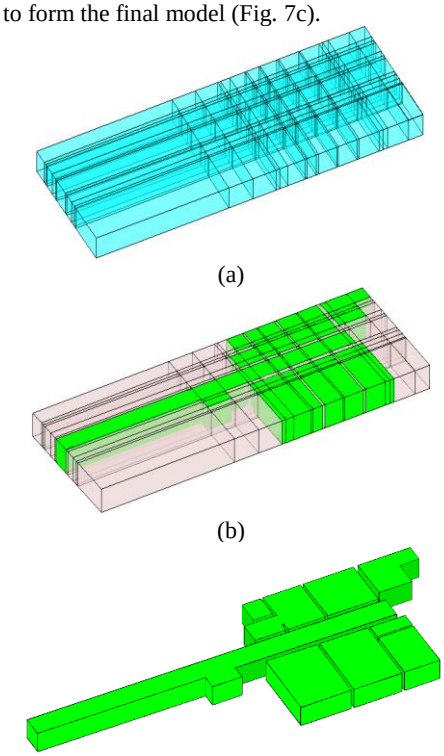

(a) (b) (c)

Fig. 7. Results for the TUB1 dataset: (a) 3D cell decomposition, (b) the classification of cells into navigable spaces (green) and non-navigable spaces (light pink), (c) the final model.

Akin to the synthetic dataset, the adjacent navigable spaces are merged together in order to produce the final model with a low complexity. The final model, which contains a long corridor and 9 separated rooms, is interactively selected by the user. The user interaction can ensure that the most suitable model is selected as the final model among the most probable models given the input data.

We evaluate the performance of our approach by comparison between the final reconstructed model and the ground truth building spaces of TUB1 which is generated manually by an expert (Khoshelham et al., 2017). Fig. 8 shows the ground truth interior space of the building TUB1.

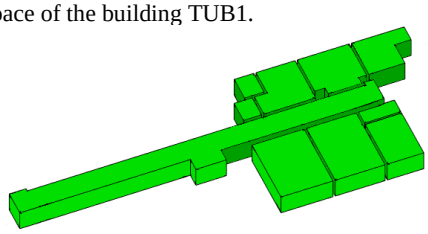

Fig. 8. The ground truth interior space of the TUB1 dataset

It can be seen by visual inspection that the majority of the building spaces are reconstructed in the final model. The total area of surfaces bounding the rooms and the corridor in the final model is about 967 m^2 in comparison with about 978 m^2 for the ground truth model. A quantitative evaluation of the final reconstructed model in comparison with the ground truth based on the framework proposed by Khoshelham et al. (2018) reveals that the model is reconstructed with a high completeness ($M_{Comp} > 92\%$) and a high correctness ($M_{Corr} > 92\%$). However, about 10% of the surfaces bounding navigable spaces are reconstructed with a large deviation (buffer size $> 15cm$). The median absolute distance between surfaces in the final model and their corresponding ones in ground truth is about $M_{Acc} \approx 2.65\ cm$. The quantitative evaluation of the final model in terms of completeness M_{Comp}, correctness M_{Corr}, and accuracy M_{Acc} is shown in detail in Fig. 9.

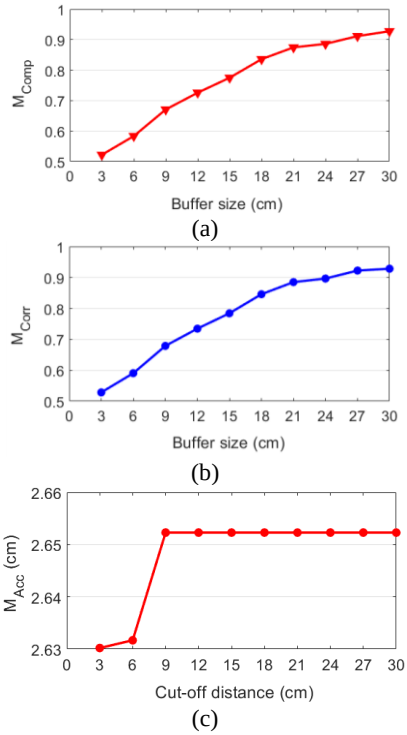

(a) (b) (c)

Fig. 9. Quality evaluation of the 3D model of the interior space of the TUB1 building: (a) Completeness; (b) Correctness; (c) Accuracy.

5. CONCLUSION AND FUTURE WORK

In this paper, we presented a stochastic approach to reconstruct 3D models of building interiors from point clouds using the rjMCMC with the Metropolis-Hastings algorithm. We take advantages of not only input data, but also the intermediate stages of the model to reconstruct the final model. The initial experiments on both a synthetic and a real dataset demonstrate the potential of our method, which can be applicable to both Manhattan and non-Manhattan architectures, as well as to incomplete and inaccurate data.

Currently, our method can reconstruct navigable spaces (i.e., rooms, corridors) of indoor environments. The building structures are considered as the surfaces of these navigable spaces. Future work will extend the method to reconstruct volumetric building elements (i.e., walls, ceiling, floors) as well as the topological relations between spaces. We will further evaluate our method with more complicated indoor environments and with higher level of clutter and occlusions.

ACKNOWLEDGEMENTS

The first author acknowledges the financial support from the University of Melbourne through Melbourne International Fee Remission and a Melbourne International Research Scholarship. The support by the Australian Research Council grant DP170100109 is also acknowledged. The datasets used in the experiments were collected as part of the ISPRS Benchmark on Indoor Modelling.

REFERENCES

Adan, A., Huber, D., 2011. 3D reconstruction of interior wall surfaces under occlusion and clutter. International Conference on 3D Imaging, Modeling, Processing, Visualization and Transmission, IEEE Computer Society, Los Alamitos, CA, USA, 275–281.

Budroni, A. and Böhm, J., 2010. Automatic 3D modelling of indoor manhattan-world scenes from laser data. Proceedings of the International Archives of Photogrammetry, Remote Sensing and Spatial Information Sciences, pp.115-120.

Díaz-Vilariño, L., Khoshelham, K., Martínez-Sánchez, J., Arias, P., 2015. 3D modeling of building indoor spaces and closed doors from imagery and point clouds. *Sensors (Switzerland)*, 15, 3491-3512.

Edelsbrunner, H. and Mücke, E.P., 1994. Three-dimensional alpha shapes. *ACM Trans. Graph*13(1), 43–72.

Elberink, S.O. and Khoshelham, K., 2015. Automatic extraction of railroad centerlines from mobile laser scanning data. Remote sensing, 7(5), pp.5565-5583.

Elberink, S.O., Khoshelham, K., Arastounia, M. and Benito, D.D., 2013. Rail track detection and modelling in mobile laser scanner data. ISPRS Int. Arch. Photogramm. Remote Sens. Spat. Inf. Sci, pp.223-228.

Hastings, W.K., 1970. Monte Carlo sampling methods using Markov chains and their applications. Biometrika 57(1), 97- 109.
Hong, S., Jung, J., Kim, S., Cho, H., Lee, J., Heo, J., 2015. Semi-automated approach to indoor mapping for 3d as-built building information modeling. *Computers, Environment and Urban Systems*, 51, 34-46.

Khoshelham, K., 2018. Smart Heritage: Challenges in Digitisation and Spatial Information Modelling of Historical Buildings. 2nd Workshop On Computing Techniques For Spatio-Temporal Data in Archaeology And Cultural Heritage, Melbourne, Australia.

Khoshelham, K. and Díaz-Vilariño, L., 2014. 3D modeling of interior spaces: learning the language of indoor architecture, ISPRS Technical Commission V Symposium "Close-range imaging, ranging and applications", Riva del Garda, Italy.

Khoshelham, K., Díaz Vilariño, L., Peter, M., Kang, Z., Acharya, D., 2017. “The ISPRS Benchmark on Indoor Modelling.” The International Archives of Photogrammetry, Remote Sensing and Spatial Information Sciences XLII-2/W7, 367-372.

Macher, H., Landes, T., Grussenmeyer, P., 2017. “From Point Clouds to Building Information Models: 3D Semi-Automatic Reconstruction of Indoors of Existing Buildings.” Applied Sciences, 7, 1030. Doi: 10.3390/app7101030

Merrell, P., Schkufza, E. and Koltun, V., 2010. Computer-generated residential building layouts. In ACM Transactions on Graphics, Vol. 29, No. 6, p. 181.

Mura, C., Mattausch, O., Pajarola, R., 2016. Piecewise-planar Reconstruction of Multi-room Interiors with Arbitrary Wall Arrangements. Computer Graphics Forum. Wiley Online Library, 179-188.

Nikoohemat, S., Peter, M., Oude Elberink, S., Vosselman, G., 2018. Semantic Interpretation of Mobile Laser Scanner Point Clouds in Indoor Scenes Using Trajectories. Remote sensing, 10(11), p.1754.

Oesau, S., Lafarge, F., Alliez, P., 2014. Indoor scene reconstruction using feature sensitive primitive extraction and graph-cut. *ISPRS Journal of Photogrammetry and Remote Sensing* 90(0), 68-82.

Pătrăucean, V., Armeni, I., Nahangi, M., Yeung, J., Brilakis, I., Haas, C., 2015. “State of research in automatic as-built modelling.” Advanced Engineering Informatics, 29, 162-171.

Ripperda, N. and Brenner, C., 2007. Data driven rule proposal for grammar based facade reconstruction. Photogrammetric Image Analysis, 36(3/W49A), pp.1-6.

Ripperda, N. and Brenner, C., 2009, June. Application of a formal grammar to facade reconstruction in semiautomatic and automatic environments. In Proc. of the 12th AGILE Conference on GIScience (pp. 1-12).

Ripperda, N., 2008. Grammar based facade reconstruction using rjMCMC. Photogrammetrie Fernerkundung Geoinformation, (2), pp.83-92.

Sanchez, V., Zakhor, A., 2012. Planar 3D modeling of building interiors from point cloud data, 19th IEEE International Conference on Image Processing (ICIP), Orlando, FL, pp. 1777-1780.

Schmidt, A., Lafarge, F., Brenner, C., Rottensteiner, F., Heipke, C., 2017. Forest point processes for the automatic extraction of

networks in raster data. ISPRS Journal of Photogrammetry and Remote Sensing, 126, pp.38-55.

Schnabel, R., Wahl, R., Klein, R., 2007. Efficient RANSAC for point-cloud shape detection. Comput. Graph. Forum 26, 214–226.

Tran, H., Khoshelham, K., 2019. Building Change Detection Through Comparison of a Lidar Scan with a Building Information Model, ISPRS Geospatial Week 2019, Enschede, The Netherlands.

Tran, H., Khoshelham, K., Kealy, A., Díaz Vilariño, L., 2017. Extracting topological relations between indoor spaces from point clouds. ISPRS Annals of the Photogrammetry, Remote Sensing and Spatial Information Sciences 4, 401- 406.

Tran, H., Khoshelham, K., Kealy, A., Díaz-Vilariño, L., 2018. Shape Grammar Approach to 3D Modelling of Indoor Environments Using Point Clouds. Journal of Computing in Civil Engineering In Press.

Xiao, J. and Furukawa, Y., 2012. Reconstructing the world's museums. Proceedings of the 12th European conference on Computer Vision - Volume Part I, Florence, Italy.

Xiong, X., Adan, A., Akinci, B., Huber, D., 2013. Automatic creation of semantically rich 3D building models from laser scanner data. *Automation in Construction* 31(0), 325-337.